

Existence of excitonic insulator phase in the extended Falicov-Kimball model: SO(2)-invariant slave-boson approach

B. Zenker,¹ D. Ihle,² F. X. Bronold,¹ and H. Fehske¹¹*Institut für Physik, Ernst-Moritz-Arndt-Universität Greifswald, 17489 Greifswald, Germany*²*Institut für Theoretische Physik, Universität Leipzig, 04109 Leipzig, Germany*

(Received 15 December 2009; published 16 March 2010)

We re-examine the three-dimensional spinless Falicov-Kimball model with dispersive f electrons at half filling, addressing the dispute about the formation of an excitonic condensate, which is closely related to the problem of electronic ferroelectricity. To this end, we work out a slave-boson functional integral representation of the suchlike extended Falicov-Kimball model that preserves the $SO(2) \otimes U(1)^{\otimes 2}$ invariance of the action. We find a spontaneous pairing of c electrons with f holes, building an excitonic insulator state at low temperatures, also for the case of initially nondegenerate orbitals. This is in contrast to recent predictions of scalar slave-boson mean-field theory but corroborates previous Hartree-Fock and random-phase approximation results. Our more precise treatment of correlation effects, however, leads to a substantial reduction in the critical temperature. The different behavior of the partial densities of states in the weak and strong interorbital Coulomb interaction regimes supports a BCS-Bose-Einstein condensate transition scenario.

DOI: [10.1103/PhysRevB.81.115122](https://doi.org/10.1103/PhysRevB.81.115122)

PACS number(s): 71.28.+d, 71.35.Lk, 71.30.+h

I. INTRODUCTION

The excitonic instability in solids is driven by the Coulomb attraction between electrons and holes which under certain conditions causes them to form bound states. At the semimetal-semiconductor transition the conventional ground state of the crystal may become unstable with respect to the spontaneous formation of excitons. Starting from a semimetal with a sufficiently small number of electrons and holes, such that the Coulomb interaction is basically unscreened, the number of free carriers will vary discontinuously under an applied perturbation,¹ signaling a phase transition. Approaching the transition from the semiconductor side, an anomaly occurs when the (indirect) band gap, tuned, e.g., by external pressure, becomes less than the exciton binding energy.² As a consequence, a new distorted phase of the crystal, with spontaneous coherence between conduction and valence bands and a gap for charged excitations, develops. It separates, below a critical temperature, the semimetal from the semiconductor. This state, known as “excitonic insulator” (EI), can be regarded as an electron-hole pair (exciton) condensate.³ By nature, depending on from which side of the semimetal-semiconductor transition the EI is approached, the EI typifies either as a BCS condensate of loosely bound electron-hole pairs or as a Bose-Einstein condensate (BEC) of preformed tightly bound excitons.^{4–6}

The mean-field description of the EI phase is very similar to the BCS theory of superconductivity and has been worked out long-time ago.^{7–12} In this context also the transition from BCS to BE condensation was discussed.^{4,13–15} Surprisingly enough, the quantitative semimetal-EI-semiconductor phase diagram has been determined only quite recently.^{15–17} All these investigations, having normal (excited) semiconductor systems in mind, rest on the standard effective-mass Mott-Wannier-type exciton model. Thereby important band-structure and correlation effects, as well as the exciton-excitation and exciton-phonon interaction, and the intervalley scattering of excitons were largely neglected.

In nature, the EI state is evidently rare. One obstacle for creating an excitonic condensate is the far-off-equilibrium situation caused by optical excitation of excitons. But also in thermal equilibrium situations, EI states are expected to occur only under very particular circumstances, e.g., if conduction and valence bands are adequately nested.¹⁸ Actual materials experimentally studied from the viewpoint of the EI are numbered. One recent example is quasi-one-dimensional Ta₂NiSe₅ with highly polarizable Se, where angle-resolved photoemission spectra reveal an extreme valence-band top flattening indicating that the ground state might be viewed as an EI.¹⁹ At present, the transition-metal dichalcogenide 1T-TiSe₂ seems to be the only candidate for a low-temperature phase transition to the EI without the influence of any external parameters other than the temperature. Here the onset of an EI phase was invoked as driving force for the charge-density-wave transition.^{20,21} Semiconducting, pressure-sensitive mixed-valence materials, such as TmSe_{0.45}Te_{0.55}, are further candidates for exciton condensation. Fine tuning the excitonic level to the narrow $4f$ valence band, a rather large number of about 10^{20} – 10^{21} cm⁻³ (small-to-intermediate sized) excitons can be created, which presumably condense into an EI state, at temperatures below 20 K in the pressure range between 5 and 11 kbar.^{22–24} Clearly, for these rather complex transition-metal/rare-earth compounds with strong electronic correlations, simple effective-mass-model-based theories will be too crude.

The investigation of Falicov-Kimball-type models offers another promising route toward the theoretical description of the EI scenario. In its original form, the Falicov-Kimball model^{25,26} contains two types of fermions: localized f electrons and itinerant c electrons with orbital energies E_f and E_c , respectively. An on-site Coulomb interaction U of both species determines the distribution of the electrons between the f and c subsystems, and therefore may drive a valence transition, provided there is a way to establish f - c coherence. At first glance this can only be achieved by including a hybridization of the f and c bands.^{27,28} It has been shown, how-

ever, that a finite f bandwidth, being certainly more realistic than entirely localized f electrons, will also induce f - c transitions.^{29,30} The model with direct c - c and f - f hopping ($\propto t_{cf}$), is sometimes called extended Falicov-Kimball model (EFKM), the Hamiltonian of which takes the form

$$H = E_c \sum_i c_i^\dagger c_i + t_c \sum_{\langle i,j \rangle} c_i^\dagger c_j + E_f \sum_i f_i^\dagger f_i + t_f \sum_{\langle i,j \rangle} f_i^\dagger f_j + U \sum_i n_{ic} n_{if}. \quad (1)$$

Here f_i^\dagger (c_i^\dagger) creates an f (c) electron at lattice site i and $n_{if} = f_i^\dagger f_i$ ($n_{ic} = c_i^\dagger c_i$) are the corresponding number operators. Let us emphasize that the f and c bands involved have different parity.²⁹ For $t_f t_c < 0$ ($t_f t_c > 0$), we may have a direct (indirect) band gap. For $t_f \equiv 0$ (dispersionless f band), the local f electron number is strictly conserved.³¹

In the past few years, both the Falicov-Kimball model with hybridization^{27,28,32–34} and the EFKM (Refs. 29–31 and 35) have been studied in connection with the exciting idea of electronic ferroelectricity. The origin of electronic ferroelectricity is a spontaneously broken symmetry due to a nonvanishing $\langle c^\dagger f \rangle$ average, which causes finite electrical polarizability without an external, interband-transition driving field. As $\langle c^\dagger f \rangle$ is basically an excitonic expectation value, indicating the pairing of c electrons with f holes, the problem of electronic ferroelectricity is intimately connected with the appearance of an excitonic condensate. Accordingly, the question whether the ground-state phase diagram of the EFKM exhibits an EI state has attracted much attention. By means of constrained path Monte Carlo (CPMC) techniques the $T=0$ phase diagram of the EFKM was determined in one and two dimensions in the strong- and intermediate-coupling regimes.^{29,30} In both cases a ferroelectric phase was detected. A subsequent Hartree-Fock calculation shows that the mean-field phase diagram of the two-dimensional (2D) EFKM agrees even quantitatively with the CPMC data,³⁵ supporting the applicability of Hartree-Fock and RPA schemes to three- and infinite-dimensional systems.^{31,35,36} Surprisingly, the more sophisticated scalar slave-boson theory failed to find the EI phase when the f and c orbitals are nondegenerate.³⁷ The continued controversy, regarding the existence of the EI phase in the EFKM, motivates us to re-examine the problem using an improved auxiliary boson approach that ensures the rotational and gauge symmetries of the EFKM within a functional integral scheme.

II. SLAVE-BOSON THEORY

A. Slave-boson Hamiltonian

The extended Falicov-Kimball Hamiltonian (1) can be rewritten as an asymmetric Hubbard model if the orbital flavor (f, c) is represented by a pseudospin variable ($\sigma = \uparrow, \downarrow$). Using the spinor representation

$$\mathbf{a}_i = \begin{pmatrix} a_{i\uparrow} \\ a_{i\downarrow} \end{pmatrix}, \quad \mathbf{a}_i^\dagger = (a_{i\uparrow}^\dagger, a_{i\downarrow}^\dagger), \quad t = \begin{pmatrix} \kappa & 0 \\ 0 & 1 \end{pmatrix}, \quad (2)$$

where the vectors \mathbf{a}_i (\mathbf{a}_i^\dagger) are built up by the fermion annihilation (creation) operators $a_{i\uparrow}^{(\dagger)} \equiv f_i^{(\dagger)}$ and $a_{i\downarrow}^{(\dagger)} \equiv c_i^{(\dagger)}$, H becomes

$$H = \sum_{i\sigma} E_\sigma a_{i\sigma}^\dagger a_{i\sigma} + \sum_{\langle i,j \rangle} \mathbf{a}_i^\dagger t \mathbf{a}_j + U \sum_i n_{i\downarrow} n_{i\uparrow}. \quad (3)$$

In Eq. (2), $\kappa = t_\uparrow / t_\downarrow$ gives the ratio of the f and c bandwidths ($t_\downarrow = 1$ fixes the unit of energy). Obviously, the usual Hubbard model follows for $E_\uparrow = E_\downarrow$ and $\kappa = 1$. Without loss of generality we choose $E_\downarrow = 0$ and $E_\uparrow \leq 0$ in what follows.

Now the slave-boson representation of the EFKM is constructed by replacing the fermionic Hilbert space by an enlarged one of pseudofermionic and bosonic states. The local states, representing the original physical states of the EFKM, Eq. (1), in the enlarged Hilbert space in a one-to-one manner, can be created in the following way:

$$|0_i\rangle \rightarrow e_i^\dagger |\text{vac}\rangle, \quad (4)$$

$$|2_i\rangle \rightarrow \tilde{a}_{i\uparrow}^\dagger \tilde{a}_{i\downarrow}^\dagger d_i^\dagger |\text{vac}\rangle, \quad (5)$$

$$|\sigma_i\rangle \rightarrow \sum_p \tilde{a}_{i\rho}^\dagger p_{i\rho\sigma}^\dagger |\text{vac}\rangle. \quad (6)$$

The pseudofermions $\tilde{a}_{i\rho}$ satisfy anticommutation rules $\{\tilde{a}_{i\rho}, \tilde{a}_{j\rho'}^\dagger\} = \delta_{ij} \delta_{\rho\rho'}$, while usual Bose commutation rules hold for the slave bosons: $[e_i, e_j^\dagger] = \delta_{ij}$, $[p_{i\rho_1\rho_2}, p_{j\rho_3\rho_4}^\dagger] = \frac{1}{2} \delta_{ij} \delta_{\rho_1\rho_4} \delta_{\rho_2\rho_3}$, and $[d_i, d_j^\dagger] = \delta_{ij}$. The boson number operators, $e_i^\dagger e_i$, $2 \text{Tr} p_i^\dagger p_i$, and $d_i^\dagger d_i$ project on an empty, a singly occupied and a doubly occupied, and state, respectively. By introducing a slave-boson matrix operator for the case of single occupancy, $p_i^{(\dagger)}$, we adapt the spin-rotation-invariant slave-boson formulation of the Hubbard model³⁸ (for a generalization to multiorbital models see Ref. 39), in order to avoid difficulties that may arise from the scalar nature of the p_σ bosons in approximative treatments.^{37,40} The decomposition

$$p_i^{(\dagger)} = \frac{1}{2} \sum_{\mu=0}^3 \tau_\mu p_{i\mu}^{(\dagger)} \quad (7)$$

into scalar (singlet) $p_{i0}^{(\dagger)}$ and vector (triplet) $\vec{p}_i^{(\dagger)} = (p_{ix}^{(\dagger)}, p_{iy}^{(\dagger)}, p_{iz}^{(\dagger)})$ components, where τ_0 is the unity matrix and $\vec{\tau}$ the vector of Pauli spin matrices, is given as

$$p_i^{(\dagger)} = \frac{1}{2} \begin{pmatrix} p_{i0}^{(\dagger)} + p_{iz}^{(\dagger)} & p_{ix}^{(\dagger)} - i p_{iy}^{(\dagger)} \\ p_{ix}^{(\dagger)} + i p_{iy}^{(\dagger)} & p_{i0}^{(\dagger)} - p_{iz}^{(\dagger)} \end{pmatrix}. \quad (8)$$

Of course, it is crucial to select out of the extended fermion-boson Fock space the physical states. This can be achieved by imposing two sets of local constraints,

$$C_i^{(1)} = e_i^\dagger e_i + 2 \text{Tr} p_i^\dagger p_i + d_i^\dagger d_i - 1 = 0, \quad (9)$$

$$C_i^{(2)} = \tilde{\mathbf{a}}_i \otimes \tilde{\mathbf{a}}_i^\dagger + 2 p_i^\dagger p_i + d_i^\dagger d_i \tau_0 - \tau_0 = 0. \quad (10)$$

$C_i^{(1)}$ expresses the completeness of the bosonic operators, i.e., each lattice site i can only be occupied by exactly one boson. $C_i^{(2)}$ relates the pseudofermion number to the number of p and d bosons.

Correspondingly, the mapping of the physical electron operators into products of new pseudofermions and slave bosons in the hopping term of H is

$$\mathbf{a}_i \rightarrow \underline{z}_i \tilde{\mathbf{a}}_i. \quad (11)$$

The choice of the hopping operators \underline{z}_i is not unique. This arbitrariness can be used, e.g., to reproduce, for the Hubbard model case, the correct free-fermion result at $U=0$ and the Gutzwiller result for any finite U at the mean-field level, where the constraints, Eqs. (9) and (10), are fulfilled only on the average. This is guaranteed by choosing^{38,41}

$$\underline{z}_i = L_i e_i^\dagger M_i p_i N_i + L_i \tilde{p}_i^\dagger M_i d_i N_i \quad (12)$$

with

$$L_i = [(1 - d_i^\dagger d_i) \mathcal{T}_0 - 2 p_i^\dagger p_i]^{-1/2}, \quad (13)$$

$$N_i = [(1 - e_i^\dagger e_i) \mathcal{T}_0 - 2 \tilde{p}_i^\dagger \tilde{p}_i]^{-1/2}, \quad (14)$$

$$M_i = [1 + e_i^\dagger e_i + d_i^\dagger d_i + 2 \text{Tr } p_i^\dagger p_i]^{1/2}, \quad (15)$$

and $\tilde{p}_{i\rho\rho'}^{(\dagger)} = \rho\rho' p_{i-\rho'-\rho}^{(\dagger)}$. The Hubbard interaction term of H can be bosonized via

$$n_{i\uparrow} n_{i\downarrow} \rightarrow d_i^\dagger d_i. \quad (16)$$

That is, the transformation to slave-boson fields results in a linearization of the interaction and we end up with the EFKM Hamiltonian in the form

$$H = \frac{E_\uparrow}{2} \sum_i \tilde{\mathbf{a}}_i^\dagger (\mathcal{T}_0 + \mathcal{T}_z) \tilde{\mathbf{a}}_i + \sum_{\langle i,j \rangle} \tilde{\mathbf{a}}_i^\dagger \underline{t}_{ij} \tilde{\mathbf{a}}_j + U \sum_i d_i^\dagger d_i. \quad (17)$$

B. Functional integral representation

To proceed further, it is convenient to represent the grand canonical partition function of the constrained system (17), $Z = \text{Tr } e^{-\beta(H - \mu N_e)}$, as an imaginary-time path integral over Grassmann fermionic and complex bosonic fields⁴²

$$Z = \int D[\tilde{\mathbf{a}}_\rho, \tilde{\mathbf{a}}_\rho] D[e^*, e] D[p_\mu^*, p_\mu] D[d^*, d] d[\lambda^{(1)}] d[\lambda_\mu^{(2)}] \times e^{-\int_0^\beta d\tau L(\tau)} \quad (18)$$

with the Lagrangian

$$\begin{aligned} L(\tau) = & \sum_i [-\lambda_i^{(1)} + e_i^* (\partial_\tau + \lambda_i^{(1)}) e_i + 2 \text{Tr } p_i^{*T} ((\partial_\tau + \lambda_i^{(1)}) \mathcal{T}_0 \\ & - \lambda_i^{(2)T}) p_i^T + d_i^* (\partial_\tau + \lambda_i^{(1)} + U - \text{Tr } \lambda_i^{(2)}) d_i] \\ & + \sum_i \tilde{\mathbf{a}}_i \left((\partial_\tau - \mu) \mathcal{T}_0 + \lambda_i^{(2)} + \frac{E_\uparrow}{2} (\mathcal{T}_0 + \mathcal{T}_z) \right) \tilde{\mathbf{a}}_i \\ & + \sum_{\langle i,j \rangle} \tilde{\mathbf{a}}_i \underline{z}_{ij}^* \tilde{\mathbf{a}}_j. \end{aligned} \quad (19)$$

Here $\beta=1/T$ is the inverse temperature and the time-independent Lagrange multipliers $\lambda_i^{(1)}$, $\lambda_i^{(2)} = \lambda_{i0}^{(2)} \mathcal{T}_0 + \lambda_{iz}^{(2)} \mathcal{T}_z$ are introduced to enforce the constraints via the integral representation of the δ function,⁴³

$$\delta[C^{(l)}] = \frac{\beta}{2\pi i} \int_c^{c+2\pi i/\beta} d\lambda^{(l)} e^{-\beta \lambda^{(l)} C^{(l)}} \quad (20)$$

(the path of the λ integration is parallel to the imaginary axis and one finds $\lambda \in \mathbf{R}^+$ at the physical saddle point).

Next, exploiting the gauge symmetry of the action, we perform local time-dependent phase transformations,

$$e_i \rightarrow e_i e^{-i\vartheta_i}, \quad (21)$$

$$d_i \rightarrow d_i e^{-i\psi_i}, \quad (22)$$

$$p_i \rightarrow p_i e^{-i(\chi_{i0} \mathcal{T}_0 - \chi_{iz} \mathcal{T}_z)}, \quad (23)$$

$$\tilde{\mathbf{a}}_i \rightarrow \tilde{\mathbf{a}}_i e^{-i(\varphi_{i0} \mathcal{T}_0 - \varphi_{iz} \mathcal{T}_z)}. \quad (24)$$

Note that both the original as well as the transformed Bose fields are complex. By the transformation, Eq. (24), the kinetic contribution generates extra terms violating the $\text{SO}(2) \otimes \text{U}(1)^{\otimes 3}$ invariance of the model. Transforming the Lagrange multipliers into real time-dependent Bose fields,

$$\lambda_i^{(1)} \rightarrow \lambda_i^{(1)} + i\vartheta_i, \quad (25)$$

$$\lambda_i^{(2)} \rightarrow e^{i(\chi_{i0} \mathcal{T}_0 - \chi_{iz} \mathcal{T}_z)} \lambda_i^{(2)} e^{-i(\chi_{i0} \mathcal{T}_0 - \chi_{iz} \mathcal{T}_z)} - i(\dot{\chi}_{i0} \mathcal{T}_0 - \dot{\chi}_{iz} \mathcal{T}_z) + i\dot{\vartheta}_i \mathcal{T}_0, \quad (26)$$

and, in addition, restricting the phase transformation to $\text{SO}(2) \otimes \text{U}(1)^{\otimes 2}$ symmetry by

$$\psi_i = 2\chi_{i0} - \vartheta_i, \quad (27)$$

$$\varphi_{i0} = -\chi_{i0} + \vartheta_i, \quad (28)$$

$$\varphi_{iz} = -\chi_{iz}, \quad (29)$$

the gauge invariance of the action is satisfied. We now make use of the gauge freedom to remove three phases of the Bose fields in radial gauge, where the fields are given as modulus times a phase factor,

$$e_i \rightarrow |e_i| e^{-i\tilde{\vartheta}_i}, \quad (30)$$

$$d_i \rightarrow |d_i| e^{-i\tilde{\psi}_i}, \quad (31)$$

$$p_i \rightarrow \frac{1}{2} \sum_\mu |p_{i\mu}| \mathcal{T}_\mu e^{-i(\tilde{\chi}_{i0} \mathcal{T}_0 - \tilde{\chi}_{iz} \mathcal{T}_z)}. \quad (32)$$

As a consequence, three bosons, e.g., $e_i(\tau)$, $p_{i0}(\tau)$, and $p_{iz}(\tau)$, can be taken as real valued, i.e., their kinetic terms, being proportional to the time derivatives in Eq. (19), drop out due to the periodic boundary conditions imposed on Bose fields [$\phi_i(\beta) = \phi_i(0)$]. However, the other three bosons p_{ix} , p_{iy} , and d_i remain complex,

$$d_i \rightarrow |d_i| e^{-i\psi_i} \quad \text{with} \quad \psi_i = \tilde{\psi}_i - 2\tilde{\chi}_{i0} + \tilde{\vartheta}_i, \quad (33)$$

$$p_i \rightarrow \frac{1}{2} \begin{bmatrix} p_{i0} + p_{iz} & (|p_{ix}| - i|p_{iy}|)e^{-2i\tilde{\chi}_{iz}} \\ (|p_{ix}| + i|p_{iy}|)e^{2i\tilde{\chi}_{iz}} & p_{i0} - p_{iz} \end{bmatrix}. \quad (34)$$

This has to be contrasted to the $SU(2) \otimes U(1)$ -invariant Hubbard model (t - J model), where only one Bose field stays complex (all Bose fields become real).^{44–46}

Using the familiar Grassman integration formula,

$$\int D[\tilde{a}_\rho, \tilde{a}_\rho] e^{-\sum \tilde{a}_\rho (-G^{-1})_{\rho\rho'} \tilde{a}_\rho} = e^{\text{Tr} \ln(-G^{-1})}, \quad (35)$$

the grand canonical partition function can be represented as a functional integral over Bose fields only,

$$Z = \int D[e] D[p_0] D[p_x^*, p_x] D[p_y^*, p_y] \\ \times D[p_z] D[d^*, d] D[\lambda^{(1)}] D[\lambda_0^{(2)}] D[\tilde{\lambda}^{(2)}] e^{-S} \quad (36)$$

with the effective bosonic action

$$S = \int_0^\beta d\tau \left\{ \sum_i \left[-\lambda_i^{(1)} + \lambda_i^{(1)} e_i^2 + \sum_\mu (\lambda_i^{(1)} - \lambda_{i0}^{(2)}) |p_{i\mu}|^2 - p_{i0} (p_i^* \right. \right. \\ \left. \left. + \tilde{p}_i) \tilde{\lambda}_i^{(2)} - i\tilde{\lambda}_i^{(2)} (p_i^* \times \tilde{p}_i) + (\lambda_i^{(1)} + U - 2\lambda_{i0}^{(2)}) |d_i|^2 \right. \right. \\ \left. \left. + p_{ix}^* \partial_\tau p_{ix} + p_{iy}^* \partial_\tau p_{iy} + d_i^* \partial_\tau d_i \right] \right\} - \text{Tr} \ln[-G_{(ij),\rho\rho'}^{-1}(\tau, \tau')], \quad (37)$$

where the inverse Green propagator is given by

$$G_{(ij),\rho\rho'}^{-1}(\tau, \tau') = \left[(-\partial_\tau + \mu - \lambda_{i0}^{(2)}) \delta_{\rho\rho'} - \frac{E_\uparrow}{2} (\mathcal{I}_0 + \mathcal{I}_z)_{\rho\rho'} \right. \\ \left. - \tilde{\lambda}_i^{(2)} \tilde{\tau}_{\rho\rho'} \right] \delta_{ij} \delta(\tau - \tau') - (\tilde{z}_i^* \tilde{z}_j)_{\rho\rho', \tau\tau'} (1 - \delta_{ij}). \quad (38)$$

The trace in Eq. (37) extends over time, space, and spin variables.

The Hermitian \tilde{z}_i matrix can be brought into the form

$$\tilde{z}_i = \begin{pmatrix} |x_{i1}|^2 z_{i1} + |x_{i2}|^2 z_{i2} & x_{i1} y_{i1}^* z_{i1} + x_{i2} y_{i2}^* z_{i2} \\ x_{i1}^* y_{i1} z_{i1} + x_{i2}^* y_{i2} z_{i2} & |y_{i1}|^2 z_{i1} + |y_{i2}|^2 z_{i2} \end{pmatrix}, \quad (39)$$

where

$$\begin{pmatrix} x_{i1} \\ y_{i1} \end{pmatrix} = \frac{1}{C_{i-}} \begin{pmatrix} p_{ix} - ip_{iy} \\ p_i - p_{iz} \end{pmatrix}, \quad (40)$$

$$\begin{pmatrix} x_{i2} \\ y_{i2} \end{pmatrix} = \frac{1}{C_{i+}} \begin{pmatrix} p_{ix} - ip_{iy} \\ -p_i - p_{iz} \end{pmatrix} \quad (41)$$

are the eigenvectors of p_i , \tilde{p}_i with

$$p_i = |\tilde{p}_i| = \sqrt{|p_{ix}|^2 + |p_{iy}|^2 + p_{iz}^2}, \quad (42)$$

$$C_{i\mp} = [2p_i(p_i \mp p_{iz})]^{1/2}, \quad (43)$$

and

$$z_{i1} = \left[(1 - |d_i|^2) - \frac{1}{2}(p_{i0} + p_i)^2 \right]^{-1/2} \\ \times \frac{1}{\sqrt{2}} [e_i(p_{i0} + p_i) + d_i(p_{i0} - p_i)] \\ \times \left[(1 - e_i^2) - \frac{1}{2}(p_{i0} - p_i)^2 \right]^{-1/2}, \quad (44)$$

$$z_{i2} = \left[(1 - |d_i|^2) - \frac{1}{2}(p_{i0} - p_i)^2 \right]^{-1/2} \\ \times \frac{1}{\sqrt{2}} [e_i(p_{i0} - p_i) + d_i(p_{i0} + p_i)] \\ \times \left[(1 - e_i^2) - \frac{1}{2}(p_{i0} + p_i)^2 \right]^{-1/2}. \quad (45)$$

Then we get

$$z_{i\uparrow\downarrow} = x_{i1} y_{i1}^* (z_{i1} - z_{i2}), \quad (46)$$

$$z_{i\downarrow\uparrow} = x_{i1}^* y_{i1} (z_{i1} - z_{i2}). \quad (47)$$

We note that only for the half-filled band case ($n_\uparrow + n_\downarrow = 1$, $e_i = |d_i|$), we find that $z_{i1} = z_{i2} = z_i$, i.e.,

$$\tilde{z}_i = z_i \mathcal{I}_0 \quad (48)$$

becomes diagonal, and the matrix elements of the original Hamiltonian are reproduced by the slave-boson transformed model. That means, Eq. (36) with Eqs. (37)–(48) provide an exact representation of the partition function for the EFKM at half filling. By contrast, for the $SU(2)$ -invariant Hubbard Hamiltonian with $\kappa=1$ and $E_\uparrow=0$, the slave-boson representation of Z holds exactly for all fillings.

For the EFKM case with $t_\uparrow t_\downarrow < 0$ (direct gap in the paraphase for large $|E_\uparrow|$), the EI order parameter Δ_\perp and the ‘‘Hartree shift’’ Δ_z are, respectively, given as^{31,35,36}

$$\Delta_\perp = \frac{U}{N} \sum_i \langle a_{i\uparrow}^\dagger a_{i\uparrow} \rangle, \quad (49)$$

$$\Delta_z = \frac{U}{N} \sum_{i\sigma} \sigma \langle a_{i\sigma}^\dagger a_{i\sigma} \rangle. \quad (50)$$

Using the constraints, Eq. (10), these relations can be expressed as functional averages,

$$\Delta_\perp = \frac{U}{N} \sum_i \langle p_{i0} (p_{ix} - ip_{iy}) \rangle, \quad (51)$$

$$\Delta_z = 2 \frac{U}{N} \sum_i \langle p_{i0} p_{iz} \rangle. \quad (52)$$

C. Saddle-point approximation

The evaluation of Eq. (36) is usually carried out by a loop expansion of the collective action, Eq. (37). At the first level

of approximation, the bosonic fields are replaced by their time-averaged values, and one looks for an extremum of the bosonized action with respect to the Bose and Lagrange multiplier fields $\phi_{i\alpha}=(e_i, p_{i0}, \vec{p}_i, d_i, \lambda_i^{(1)}, \lambda_{i0}^{(2)}, \vec{\lambda}_i^{(2)})$,

$$\frac{\partial S}{\partial \phi_{i\alpha}} = 0 \rightsquigarrow \bar{S} = S|_{\phi_{i\alpha}=\bar{\phi}_{i\alpha}}. \quad (53)$$

The physically relevant saddle point $\{\bar{\phi}_{i\alpha}\}$ is determined to give the lowest free energy (per site),

$$\bar{f} = \bar{\Omega}/N + \mu n, \quad (54)$$

where, at given mean electron density $n=n_\uparrow+n_\downarrow$, the chemical potential μ is fixed by the requirement

$$n = -\frac{1}{N} \frac{\partial \bar{\Omega}}{\partial \mu}. \quad (55)$$

$\bar{\Omega}=\bar{S}/\beta$ denotes the grand canonical potential. Clearly, an unrestricted minimization of the free energy is impossible for an infinite system, even within the static approximation. Focusing on the possible existence of the EI phase, we consider only uniform solutions hereafter: $\{\bar{\phi}_{i\alpha}\}=\{\bar{\phi}_\alpha\}$. Note that the inclusion of a charge-density-wave phase is straightforward, e.g., by adapting the two-sublattice slave-boson treatment worked out for the Peierls-Hubbard model.^{46–48}

Examining a tight-binding direct-band-gap situation in three dimensions, we have

$$\vec{z}^* \varepsilon_{\vec{k}} \vec{z} = z^2 \gamma_{\vec{k}} t \quad (56)$$

with

$$z^2 = \frac{2p_0^2 d^2}{\left[1 - d^2 - \frac{1}{2}(p_0 + p)^2\right] \left[1 - d^2 - \frac{1}{2}(p_0 - p)^2\right]} \quad (57)$$

and

$$\gamma_{\vec{k}} = -2[\cos k_x + \cos k_y + \cos k_z]. \quad (58)$$

The trace in Eq. (37) can be easily performed in the momentum-frequency domain after diagonalizing the propagator in pseudospin space. Then the free-energy functional takes the form

$$f[\phi_\alpha] = \lambda^{(1)}(e^2 + p_0^2 + p^2 + d^2 - 1) - 2\lambda_\perp^{(2)} p_0 p_\perp - 2\lambda_z^{(2)} p_0 p_z + U d^2 + \frac{1}{\beta N} \sum_{\vec{k}\nu} \ln[1 - n_{\vec{k}\nu}] + \tilde{\mu} n, \quad (59)$$

where

$$n_{\vec{k}\nu} = [\exp\{\beta(E_{\vec{k}\nu} - \tilde{\mu})\} + 1]^{-1} \quad (60)$$

holds with the quasiparticle energies ($\nu=\pm$),

$$E_{\vec{k}\nu} = \frac{1}{2}[E_\uparrow + (\kappa + 1)z^2 \gamma_{\vec{k}}] + \nu \sqrt{\frac{1}{4}[E_\uparrow + 2\lambda_z^{(2)} + (\kappa - 1)z^2 \gamma_{\vec{k}}]^2 + (\lambda_\perp^{(2)})^2}. \quad (61)$$

Here we have introduced $\lambda_\perp^{(2)} = \pm \sqrt{(\lambda_x^{(2)})^2 + (\lambda_y^{(2)})^2}$, $p_\perp = \mp \sqrt{p_x^2 + p_y^2}$, and $\tilde{\mu} = \mu - \lambda_0^{(2)}$.

Requiring that f becomes stationary with respect to the variation in the ϕ_α we obtain the following set of saddle-point equations,

$$\lambda_z^{(2)} = \frac{1}{2} \frac{p_z}{p_0} \left(\frac{z^2}{2d^2} - \frac{1}{p_0^2 - p^2} \right) z^2 I, \quad (62)$$

$$\lambda_\perp^{(2)} = \frac{1}{2} \frac{p_\perp}{p_0} \left(\frac{z^2}{2d^2} - \frac{1}{p_0^2 - p^2} \right) z^2 I, \quad (63)$$

$$p_0 p_z = \frac{1}{2} \frac{1}{N} \sum_{\vec{k}\nu} \nu m_{\vec{k}} n_{\vec{k}\nu}, \quad (64)$$

$$p_0 p_\perp = \frac{1}{2} \frac{1}{N} \sum_{\vec{k}\nu} \nu M_{\vec{k}} n_{\vec{k}\nu}, \quad (65)$$

$$p_0^2 = \frac{1}{2} + \frac{1}{2} \sqrt{(1 - z^2)(1 - 4p_0^2 p^2)}, \quad (66)$$

$$d^2 = \frac{1}{2z^2} \left[z^2(2 - p_0^2 - p^2) + 2p_0^2 - 2p_0 \sqrt{z^2(2 - p_0^2 - p^2) + z^4 p^2 + p_0^2} \right], \quad (67)$$

$$U + 2\lambda_\perp^{(2)} \frac{p_\perp}{p_0} + 2\lambda_z^{(2)} \frac{p_z}{p_0} = \frac{2d^2 - p_0^2 + z^2 p^2}{2p_0^2 d^2} z^2 I \quad (68)$$

with

$$I = (\kappa + 1) \frac{1}{N} \sum_{\vec{k}\nu} \gamma_{\vec{k}} n_{\vec{k}\nu} + (\kappa - 1) \frac{1}{N} \sum_{\vec{k}\nu} \nu m_{\vec{k}} \gamma_{\vec{k}} n_{\vec{k}\nu}, \quad (69)$$

$$m_{\vec{k}} = \frac{E_\uparrow + 2\lambda_z^{(2)} + (\kappa - 1)z^2 \gamma_{\vec{k}}}{\sqrt{(E_\uparrow + 2\lambda_z^{(2)} + (\kappa - 1)z^2 \gamma_{\vec{k}})^2 + (2\lambda_\perp^{(2)})^2}}, \quad (70)$$

$$M_{\vec{k}} = \frac{2\lambda_\perp^{(2)}}{\sqrt{(E_\uparrow + 2\lambda_z^{(2)} + (\kappa - 1)z^2 \gamma_{\vec{k}})^2 + (2\lambda_\perp^{(2)})^2}}. \quad (71)$$

The EI order parameter, Eq. (49), and Hartree shift, Eq. (50), become

$$\Delta_\perp = U p_0 p_\perp, \quad (72)$$

$$\Delta_z = 2U p_0 p_z. \quad (73)$$

D. Zero temperature: BI to EI transition

At zero temperature, the EFKM exhibits a trivial band insulator (BI) phase of a completely filled f (empty c) band

($n=1$, $E_{\uparrow} \leq 0$), provided the Hartree gap is finite,

$$\Delta_H(T=0) = |E_{\uparrow} + 2\lambda_z^{(2)}| - 6(|\kappa| + 1) > 0. \quad (74)$$

That is to say, in the BI phase we have $d^2=0$, $n_{\uparrow}=1$, $n_{\downarrow}=0$, and in no way f - c coherence can develop: $p_{\perp} = \lambda_{\perp}^{(2)} = 0$. Then $m_{\vec{k}} = -1$ for all \vec{k} , and $n_{\vec{k}-} = 1$, $n_{\vec{k}+} = 0$ result from Eq. (60) with Eq. (61). The constraint, Eq. (10), gives, together with Eq. (64), $p_0 = p_z = 1/\sqrt{2}$, leading to $z^2 = 1$, as for a noninteracting system. At the same time, $I=0$ according to Eq. (69), and the correlation Eq. (68) reduces to $U + 2\lambda_z^{(2)} = 0$, which gives $\Delta_z = -2\lambda_z^{(2)}$ for the BI.

Looking for an instability of the BI toward an EI state, we find from Eq. (63) that $\lambda_{\perp}^{(2)} = -\Delta_{\perp}$ near the critical Coulomb interaction U_{c2} . Multiplying Eq. (65) by U , for $\Delta_{\perp} \neq 0$, we get the $T=0$ gap equation

$$1 = \frac{1}{2N} \sum_{\vec{k}} \frac{n_{\vec{k}-} - n_{\vec{k}+}}{\sqrt{\frac{1}{4}[E_{\uparrow} - \Delta_z + (\kappa - 1)\gamma_{\vec{k}}]^2 + \Delta_{\perp}^2}}, \quad (75)$$

which agrees with the Hartree-Fock result.³⁶ As a consequence, our SO(2)-invariant slave-boson approach reproduces the BI-EI phase boundary of the EFKM Hartree-Fock ground-state phase diagram.^{31,35} At least for the 2D case it has been demonstrated that this phase boundary agrees almost perfectly with that obtained by the CPMC method.^{30,35} This also applies to our SO(2)-invariant slave-boson approach, e.g., for the 2D EFKM with $\kappa = -0.3$ and $U=2$, we obtain the critical value $|E_{\uparrow,c}| = 3.23(3.26)$ for the EI-BI transition, using the 2D tight-binding (square) density of states (DOS), in comparison with $|E_{\uparrow,c}^{\text{CPMC}}| = 3.29$ (cf. Fig. 3 in Ref. 30).

E. Scalar slave-boson approach

If one contrariwise adopts the scalar slave-boson theory⁴⁰ by introducing only four auxiliary bosonic fields per site, e_i , $p_{i\sigma}$, and d_i , where $p_i^{\dagger} p_{i\uparrow}$ ($p_i^{\dagger} p_{i\downarrow}$) projects on a singly occupied f -(c -) electron site i , the p_i matrix becomes diagonal,

$$p_i = \frac{1}{2} \begin{pmatrix} p_{i0} + p_{iz} & 0 \\ 0 & p_{i0} - p_{iz} \end{pmatrix}. \quad (76)$$

That means, the ‘‘spin-flip’’ terms in Eq. (10),

$$\tilde{a}_{i\uparrow}^{\dagger} \tilde{a}_{i\downarrow} = 2p_{i\uparrow}^{\dagger} p_{i\uparrow} + 2p_{i\downarrow}^{\dagger} p_{i\uparrow}, \quad (77)$$

$$\tilde{a}_{i\downarrow}^{\dagger} \tilde{a}_{i\uparrow} = 2p_{i\uparrow}^{\dagger} p_{i\downarrow} + 2p_{i\downarrow}^{\dagger} p_{i\downarrow}, \quad (78)$$

do not occur. As these terms, in view of Eqs. (49) and (51), are essential for the formation of an excitonic insulator, the scalar slave-boson approach fails to describe the EI phase, at least for finite orbital-energy difference $E_{\uparrow} \neq 0$. At the (uniform) saddle-point level of approximation, within scalar slave-boson theory, we find the band-renormalization factor

$$z^2 = \frac{d^2(p_{\uparrow} + p_{\downarrow})^2}{n_{\uparrow} n_{\downarrow}} \quad (79)$$

with $p_{\uparrow} = \sqrt{2} p_{\uparrow\uparrow}$ ($p_{\downarrow} = \sqrt{2} p_{\downarrow\downarrow}$), and the correlation Eq. (68) simplifies to

$$U = z^2 \left(\frac{1}{p_{\uparrow} p_{\downarrow}} - \frac{1}{d^2} \right) \frac{1}{N} \sum_{\vec{k}} (\kappa \gamma_{\vec{k}} n_{\vec{k}\uparrow} + \gamma_{\vec{k}} n_{\vec{k}\downarrow}). \quad (80)$$

III. NUMERICAL RESULTS

In the numerical evaluation of the self-consistency loop, Eqs. (54)–(71), we proceed as follows: at given model parameters E_f , κ , U , and fixed total particle density $n = n_f + n_c = 1$, we solve the finite-temperature saddle-point equations for the slave-boson and Lagrange parameter fields $\{\bar{\phi}_{\alpha}\}$ together with the equation for the renormalized chemical potential $\tilde{\mu}$ using an iteration technique. Thereby \vec{k} summations were transformed into energy integrals, introducing the (tight-binding) density of states for the simple cubic lattice. Convergence is assumed to be achieved if all quantities are determined with a relative error less than 10^{-6} . Our numerical scheme allows for the investigation of different metastable states corresponding to local minima of the variational free-energy functional. Of course, we will always obtain a homogeneous, translational invariant solution without spontaneous (polarization) exciton formation. In this case the f and c bands are simply shifted by $2\lambda_z^{(2)}$, leading to a gapped band structure at large enough U . Besides these simple (semi-) metallic and BI phases, the $T=0$ Hartree-Fock ground-state phase diagram of the half-filled EFKM exhibits two symmetry-broken states:^{31,35} the anticipated EI and a charge-density-wave phase. At $E_f = E_c$ (degenerate orbitals), the charge-density-wave ground state is stable for all values of κ . It becomes rapidly suppressed, however, for $E_f \neq E_c$ (nondegenerate orbitals), in particular, if the c and f bandwidths are comparable.³⁵ As we are interested in the (uniform) EI phase only, we have confined our slave-boson approach to spatially uniform saddle points. With respect to charge-density-wave formation this will be uncritical for the parameter values studied in the following.

Figure 1 gives the slave-boson phase boundary of the EI

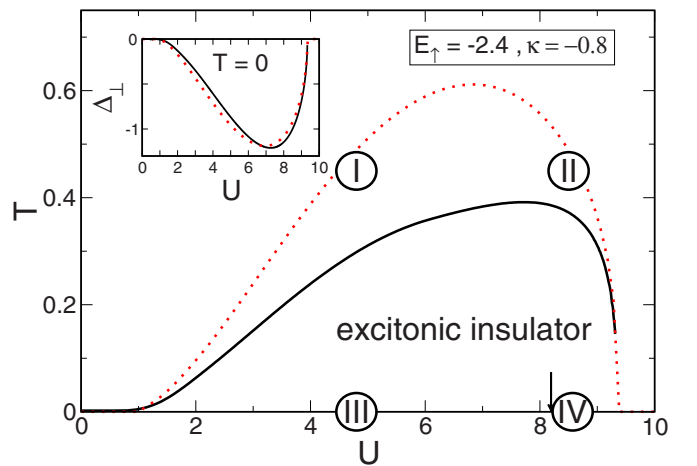


FIG. 1. (Color online) Stability region of the EI phase in the three-dimensional (3D) half-filled EFKM [the arrow marks the critical coupling where the Hartree gap, Eq. (74), opens]. The inset shows the order parameter at zero temperature. Red dotted curves give the Hartree-Fock results for comparison.

in the U - T plane, calculated for $E_{\uparrow} = -2.4$ and $\kappa = -0.8$. Most notably, we obtain a stable EI solution for the nondegenerate band case, which has to be contrasted with the result of the scalar slave-boson approach.³⁷

Let us first discuss the $T=0$ data. Here the numerical semimetal-EI and EI-BI transition points at small and large Coulomb interaction, $U_{c1} \approx 0.74$ and $U_{c2} \approx 9.3$, respectively, agree with the Hartree-Fock results (see the dotted curve). The latter was proved analytically in Sec. II D. The inset gives the U dependence of the EI order parameter at $T=0$. For $U_{c1} \leq U \leq U_{c2}$, Δ_{\perp} only slightly deviates from the corresponding Hartree-Fock curve.

The variation in the other bosonic fields is depicted in Fig. 2, where the solid curves belong to the parameter values used in Fig. 1. We see that the number of empty and double-occupied sites, e^2 and d^2 , is equal and goes to zero at the EI-BI transition, where we have $p_0^2 = p_z^2 = 1/2$ at singly occupied sites. Nonvanishing values of p_{\perp}^2 and $\lambda_{\perp}^{(2)}$ indicate an EI state, which demonstrates the importance of the (transverse) spin-flip processes for the formation and maintenance of f - c coherence. The slave-boson band shift $|2\lambda_z^{(2)}|$ in Eq. (61) increases with increasing U (just as the Hartree shift). Obviously, the area of the EI phase is enlarged if one reduces the splitting of the f and c band centers (cf. the red dot-dashed

lines). We include the data for the metastable EI solution at $E_{\uparrow} = 0$ (as discussed above, in this case the charge-density-wave state will win), in order to show that d^2 and e^2 stay finite for all U . That means, for the orbital-degenerate EFKM ($\lambda_z^{(2)} = \tilde{\mu} = 0$), our SO(2)-invariant slave-boson scheme will not give the (artificial) transition into an insulating Brinkmann-Rice-type correlated-insulator state.⁴⁹ This transition is a well-known shortcoming of the scalar slave-boson approach to the Hubbard model⁴⁰ and has been also observed applying the scalar slave-boson theory to the EFKM.³⁷ The effect becomes even more apparent by comparing the variation in the slave-boson band-renormalization factors z^2 .

Figure 3 shows that z^2 vanishes within the scalar slave-boson theory (right-hand panel) for $E_{\uparrow} = 0$ at a critical interaction strength ($U_{BR} \approx 14.5$), indicating the localization of charge carriers, whereas in our theory the bandwidth will be only slightly renormalized at this point (see left-hand panel). Interestingly, the band renormalization is rather small in the EI phase as well (cf. the curves for $E_{\uparrow} = -1.2, -2.4$). Here we find $z^2 \geq 0.95$, which explains the small deviation of the slave-boson order parameter from its Hartree-Fock counterpart (see inset of Fig. 1).

Next we discuss the finite-temperature behavior. The variation in the EI order parameter and of the band-

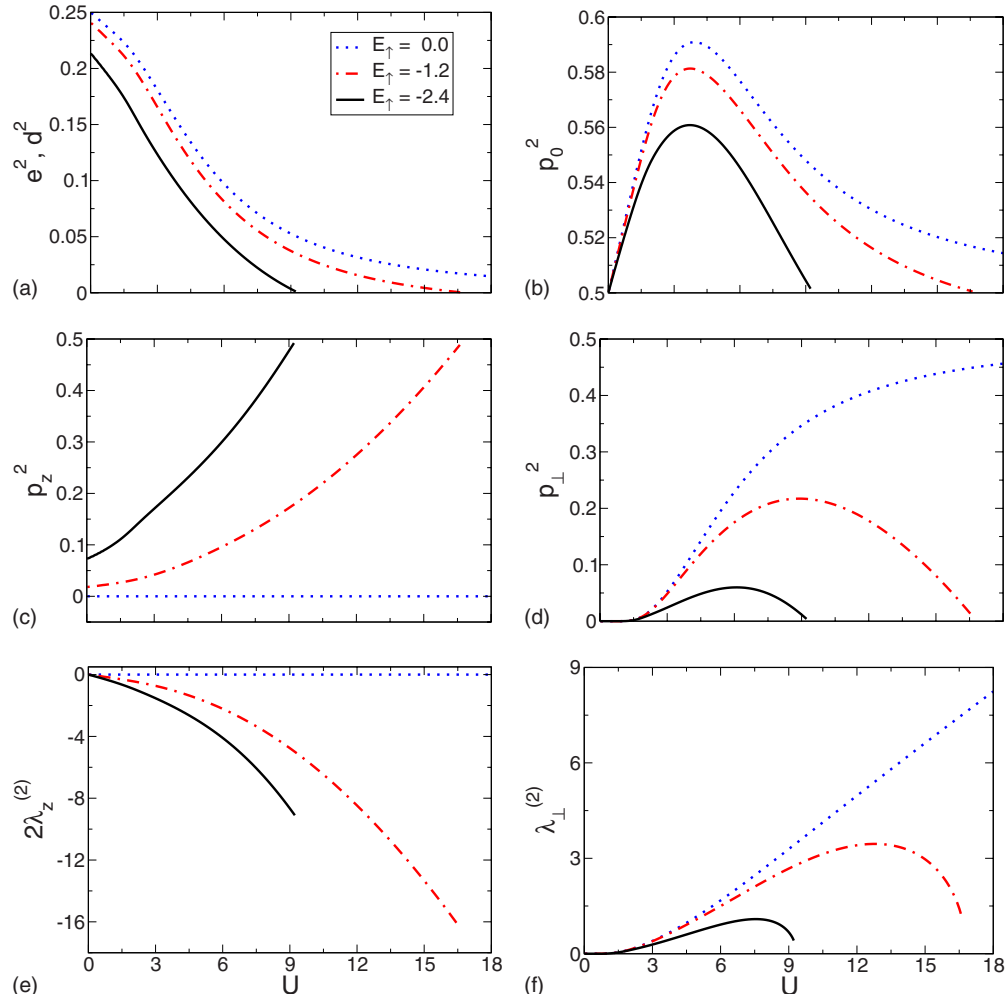


FIG. 2. (Color online) U dependence of slave-boson fields and Lagrange parameters for different E_{\uparrow} at $T=0$ ($\kappa = -0.8$).

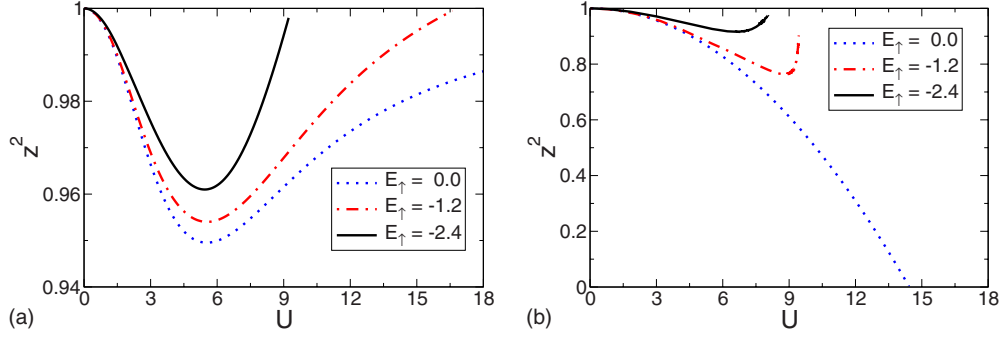


FIG. 3. (Color online) Band-renormalization factors at $T=0$ within SO(2)-invariant (left-hand panel) and scalar (right-hand panel) slave-boson theory. Again, $\kappa=-0.8$.

renormalization factor with T at fixed U is displayed in Fig. 4. Most important, in comparison with the Hartree-Fock data, the critical temperature for the EI-semimetal/semiconductor phase transition is significantly reduced (see also Fig. 1). Looking at $z^2(T)$, this may be attributed to the more precise treatment of correlations and occupation number fluctuations. At T_c , the order parameter vanishes, and we observe a cusp in z^2 . Enhancing, above T_c , the temperature further, the band renormalization goes on, where z^2 now always decreases with increasing U .

Figure 5 shows the temperature dependencies of the various slave-boson fields and Lagrange parameters for $U=6$ (corresponding to the left-hand panel of Fig. 4). As expected, p_\perp and $\lambda_\perp^{(2)}$ are monotonously decreasing functions of T , with $p_\perp(T_c)=\lambda_\perp^{(2)}(T_c)=0$. The other fields exhibit a cusp structure at T_c . At higher temperatures the probability of finding double-occupied sites and empty sites increases. At the same time, we find less singly occupied sites [$\propto(p_0^2+p_z^2)$], which means that the increase in p_0^2 is overcompensated by the reduction in p_z^2 , indicating a more balanced occupation of f and c sites.

Finally, we analyze the partial f and c electron DOS, $\rho_\uparrow(E)$ and $\rho_\downarrow(E)$, defined via

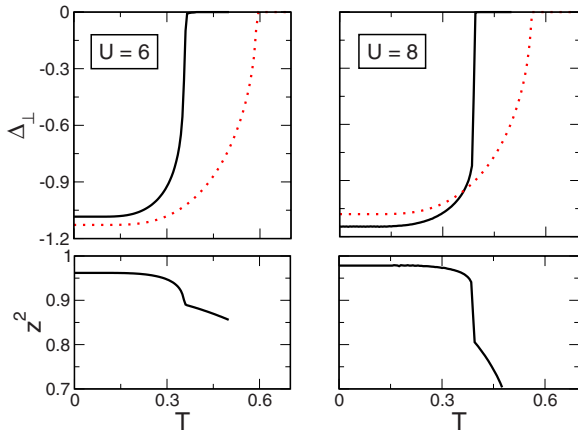


FIG. 4. (Color online) T dependence of the EI order parameter Δ_\perp and of the band renormalization z^2 at fixed Coulomb interaction $U=6$ (left-hand panels) and $U=8$ (right-hand panels). Red dotted lines show the corresponding Hartree-Fock data, where $z^2=1$. Band-structure parameters are the same as in Fig. 1.

$$n_\sigma = \frac{1}{N} \sum_{\vec{k}} n_{\vec{k}\sigma} = \int dE \rho_\sigma(E), \quad (81)$$

$$n_{\vec{k}\uparrow} = \frac{1}{2}(1+m_{\vec{k}})n_{\vec{k}+} + \frac{1}{2}(1-m_{\vec{k}})n_{\vec{k}-}, \quad (82)$$

$$n_{\vec{k}\downarrow} = \frac{1}{2}(1-m_{\vec{k}})n_{\vec{k}+} + \frac{1}{2}(1+m_{\vec{k}})n_{\vec{k}-}, \quad (83)$$

where $n_{(\vec{k})\sigma}$ are the corresponding particle densities. Figure 6 gives $\rho_{\uparrow,\downarrow}(E)$ at the characteristic U - T points marked by I–IV in the phase diagram of Fig. 1. Obviously, the high-temperature phase may be viewed as a metal/semimetal (panel I) or a small-gap semiconductor (panel II) in the weak-to-intermediate or strong Coulomb-attraction regime. Accordingly, the EI phase at low temperatures shows different characteristics as well. As can be seen from panel III, a correlation-induced “hybridization” gap opens in the DOS

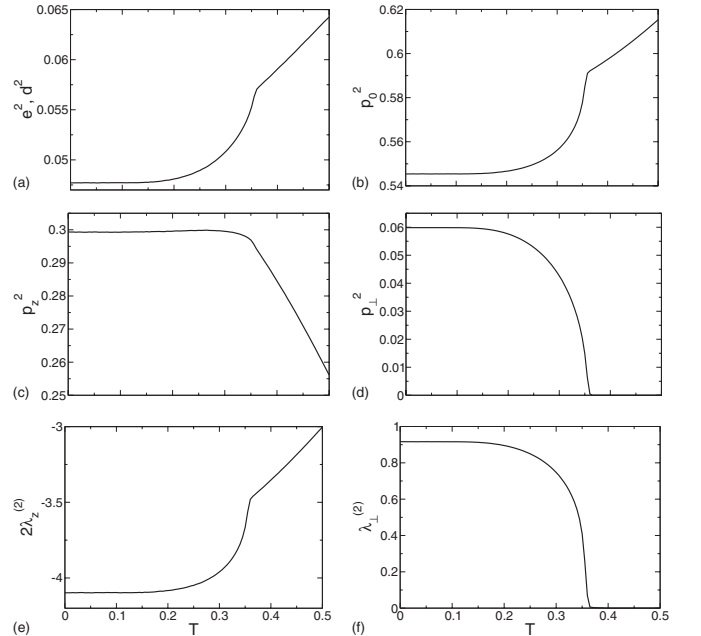


FIG. 5. T dependence of the various slave-boson fields for $U=6$, $E_f=-2.4$, and $\kappa=-0.8$.

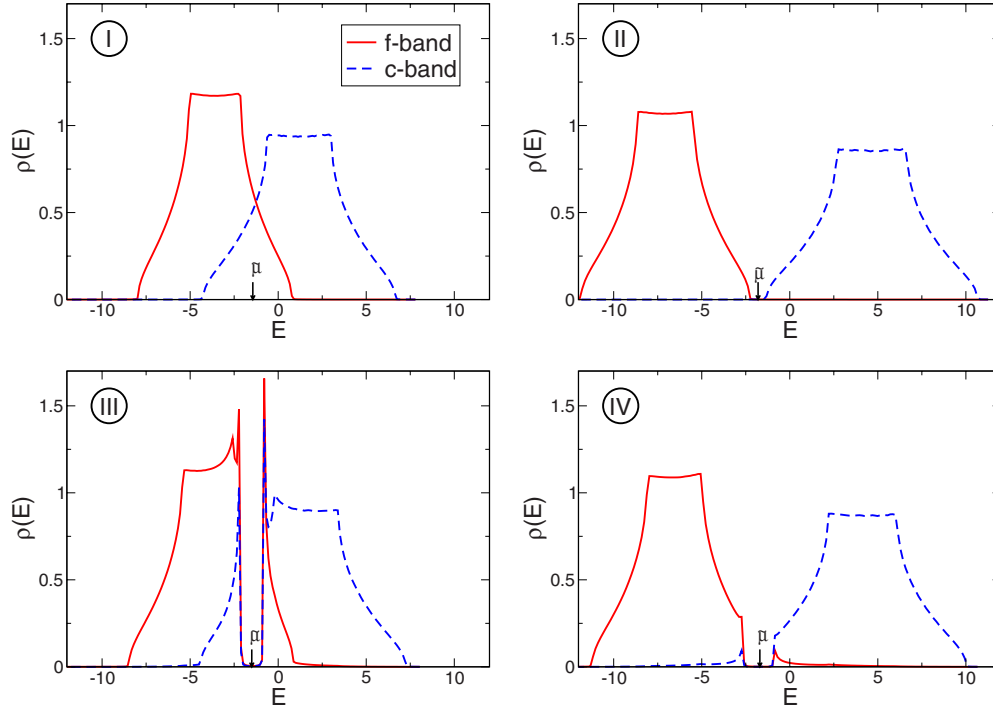


FIG. 6. (Color online) Partial densities of states for f -band (red solid curves) and c -band (blue dashed curves) electrons at the points ($U=4.8, T=0.45$), ($8.5, 0.45$), ($4.8, 0$), ($8.5, 0$) marked by I–IV in Fig. 1. Band-structure parameters are $E_f=E_c=-2.4$ and $t_f=t_c=-0.8$.

with $n_- = 1$ ($n_+ = 0$) at $T=0$, indicating EI long-range order. The pronounced c - f state mixing and strong enhancement of the DOS at the upper/lower valence/conducting band edges reminds a BCS-type pairing evolving from a (semi-) metallic state with a large Fermi surface above T_c . By contrast, the zero-temperature DOS shown in panel IV evolves from an already gapped high-temperature phase. Here, preformed pairs (excitons) may exist,^{6,36} which undergo a BEC transition at T_c .

IV. SUMMARY

In this work we studied the extended Falicov-Kimball model with respect to the formation of an exciton condensate, which is related to the problem of electronic ferroelectricity. Motivated by the discrepancy concerning the existence of the EI phase within the Hartree-Fock and scalar slave-boson approaches, we developed an $SO(2)$ -invariant slave-boson theory. The main result is that our improved slave-boson scheme is capable of describing the EI phase in a parameter region agreeing, at zero temperature, with Hartree-Fock (and, in 2D, constrained path Monte Carlo) results. This is in striking contrast to recent findings by the

scalar slave-boson approach,³⁷ which fails to detect the EI phase in the case of nondegenerate f and c orbitals. The agreement of the zero-temperature semimetal \rightarrow EI and EI \rightarrow band-insulator transition points with the Hartree-Fock and Monte Carlo values is ascribed to a rather weak band renormalization at $T=0$. At finite temperature, band-renormalization effects due to electronic correlations and particle number fluctuations become important, and, as a result, our slave-boson theory yields significantly lower transition temperatures than Hartree-Fock. From the analysis of the partial f , c , and quasiparticle densities of states, in the EI phase a crossover from a BCS-type condensate to a Bose-Einstein condensate of preformed excitons may be suggested. The results of our investigations may form the basis of forthcoming studies, e.g., on the effects of fluctuations around the saddle point, allowing the calculation of pseudospin and charge susceptibilities for the EFKM on an equal footing.

ACKNOWLEDGMENTS

The authors thank A. Alvermann, B. Bucher, N. V. Phan, G. Röpke, and H. Stolz for stimulating discussions. This work was supported by DFG through SFB 652.

¹N. F. Mott, *Philos. Mag.* **6**, 287 (1961).

²R. Knox, in *Solid State Physics*, edited by F. Seitz and D. Turnbull (Academic, New York, 1963), p. 100.

³B. I. Halperin and T. M. Rice, in *Solid State Physics*, edited by F.

Seitz, D. Turnbull, and H. Ehrenreich (Academic, New York, 1967), Vol. 21, p. 115.

⁴A. J. Leggett, in *Modern Trends in the Theory of Condensed Matter*, edited by A. Pekalski and R. Przystawa (Springer-

- Verlag, Berlin, 1980).
- ⁵C. Comte and P. Nozières, *J. Phys. (France)* **43**, 1069 (1982).
 - ⁶F. X. Bronold and H. Fehske, *Phys. Rev. B* **74**, 165107 (2006).
 - ⁷J. des Cloizeaux, *J. Phys. Chem. Solids* **26**, 259 (1965).
 - ⁸W. Kohn, in *Many Body Physics*, edited by C. de Witt and R. Balian (Gordon & Breach, New York, 1968).
 - ⁹L. V. Keldysh and H. Y. V. Kopayev, *Sov. Phys. Solid State* **6**, 2219 (1965).
 - ¹⁰A. N. Kozlov and L. A. Maksimov, *Sov. Phys. JETP* **21**, 790 (1965).
 - ¹¹D. Jérôme, T. M. Rice, and W. Kohn, *Phys. Rev.* **158**, 462 (1967).
 - ¹²J. Zittartz, *Phys. Rep.* **165**, 612 (1968).
 - ¹³P. Nozières and S. Schmitt-Rink, *J. Low Temp. Phys.* **59**, 195 (1985).
 - ¹⁴R. Zimmermann and H. Stolz, *Phys. Status Solidi B* **131**, 151 (1985).
 - ¹⁵D. Kremp, D. Semkat, and K. Henneberger, *Phys. Rev. B* **78**, 125315 (2008).
 - ¹⁶F. X. Bronold, G. Röpke, and H. Fehske, *J. Phys. Soc. Jpn. Suppl. A* **76**, 27 (2007).
 - ¹⁷F. X. Bronold and H. Fehske, *Superlattices Microstruct.* **43**, 512 (2008).
 - ¹⁸E. Bascones, A. A. Burkov, and A. H. MacDonald, *Phys. Rev. Lett.* **89**, 086401 (2002).
 - ¹⁹Y. Wakisaka, T. Sudayama, K. Takubo, T. Mizokawa, M. Arita, H. Namatame, M. Taniguchi, N. Katayama, M. Nohara, and H. Takagi, *Phys. Rev. Lett.* **103**, 026402 (2009).
 - ²⁰H. Cercellier, C. Monney, F. Clerc, C. Battaglia, L. Despont, M. G. Garnier, H. Beck, P. Aebi, L. Patthey, H. Berger, and L. Forró, *Phys. Rev. Lett.* **99**, 146403 (2007).
 - ²¹C. Monney, H. Cercellier, F. Clerc, C. Battaglia, E. F. Schwier, C. Didiot, M. G. Garnier, H. Beck, P. Aebi, H. Berger, L. Forró, and L. Patthey, *Phys. Rev. B* **79**, 045116 (2009).
 - ²²J. Neuenschwander and P. Wachter, *Phys. Rev. B* **41**, 12693 (1990).
 - ²³B. Bucher, P. Steiner, and P. Wachter, *Phys. Rev. Lett.* **67**, 2717 (1991).
 - ²⁴P. Wachter, B. Bucher, and J. Malar, *Phys. Rev. B* **69**, 094502 (2004).
 - ²⁵L. M. Falicov and J. C. Kimball, *Phys. Rev. Lett.* **22**, 997 (1969).
 - ²⁶R. Ramirez, L. M. Falicov, and J. C. Kimball, *Phys. Rev. B* **2**, 3383 (1970).
 - ²⁷K. Kanda, K. Machida, and T. Matsubara, *Solid State Commun.* **19**, 651 (1976).
 - ²⁸T. Portengen, T. Östreich, and L. J. Sham, *Phys. Rev. Lett.* **76**, 3384 (1996).
 - ²⁹C. D. Batista, *Phys. Rev. Lett.* **89**, 166403 (2002).
 - ³⁰C. D. Batista, J. E. Gubernatis, J. Bonča, and H. Q. Lin, *Phys. Rev. Lett.* **92**, 187601 (2004).
 - ³¹C. Schneider and G. Czycholl, *Eur. Phys. J. B* **64**, 43 (2008).
 - ³²T. Portengen, T. Östreich, and L. J. Sham, *Phys. Rev. B* **54**, 17452 (1996).
 - ³³G. Czycholl, *Phys. Rev. B* **59**, 2642 (1999).
 - ³⁴P. Farkašovský, *Phys. Rev. B* **59**, 9707 (1999).
 - ³⁵P. Farkašovský, *Phys. Rev. B* **77**, 155130 (2008).
 - ³⁶D. Ihle, M. Pfafferoth, E. Burovski, F. X. Bronold, and H. Fehske, *Phys. Rev. B* **78**, 193103 (2008).
 - ³⁷P. M. R. Brydon, *Phys. Rev. B* **77**, 045109 (2008).
 - ³⁸T. Li, P. Wölfle, and P. J. Hirschfeld, *Phys. Rev. B* **40**, 6817 (1989).
 - ³⁹F. Lechermann, A. Georges, G. Kotliar, and O. Parcollet, *Phys. Rev. B* **76**, 155102 (2007).
 - ⁴⁰G. Kotliar and A. E. Ruckenstein, *Phys. Rev. Lett.* **57**, 1362 (1986).
 - ⁴¹R. Frésard and P. Wölfle, *J. Phys.: Condens. Matter* **4**, 3625 (1992).
 - ⁴²J. W. Negele and H. Orland, *Quantum Many-Particle Systems* (Addison-Wesley, Reading, MA, 1988).
 - ⁴³G. Hooijer and J. E. Van Himbergen, *Phys. Rev. B* **36**, 7678 (1987).
 - ⁴⁴M. Deeg and H. Fehske, *Phys. Rev. B* **50**, 17874 (1994).
 - ⁴⁵M. Deeg, H. Fehske, and H. Büttner, *Europhys. Lett.* **26**, 109 (1994).
 - ⁴⁶H. Fehske, *Habilitationsschrift thesis*, Universität Bayreuth, 1996.
 - ⁴⁷H. Fehske, M. Deeg, and H. Büttner, *Phys. Rev. B* **46**, 3713 (1992).
 - ⁴⁸U. Trapper, H. Fehske, M. Deeg, and H. Büttner, *Z. Phys. B: Condens. Matter* **93**, 465 (1994).
 - ⁴⁹W. F. Brinkman and T. M. Rice, *Phys. Rev. B* **2**, 4302 (1970).